Protein-Surface Structural Recognition in Inactive Areas: A New Immobilization Strategy for Acetylcholinesterase

Jianxiong Diao, Xiaolu Yu, Lin Ma, Yuanqing Li, and Ying Sun

Bioconjugate Chem., **Just Accepted Manuscript** • DOI: 10.1021/acs.bioconjchem.8b00160 • Publication Date (Web): 04 Apr 2018

Protein-Surface Structural Recognition in Inactive Areas: A New Immobilization Strategy for Acetylcholinesterase

Jianxiong Diao,[†] *Xiaolu Yu,*[†] *Lin Ma,*[‡] *Yuanqing Li,*[†] *Ying Sun*[*,†]

[†] Beijing Key Laboratory of Farmland Soil Pollution Prevention and Remediation, College of Resources and Environmental Science, China Agricultural University, Beijing 100193, China.

[‡] School of Environment, Tsinghua University, Beijing 100084, China.

*Corresponding author

Beijing Key Laboratory of Farmland Soil Pollution Prevention and Remediation

College of Resources and Environmental Sciences

China Agricultural University, No. 2 Yuanmingyuan Xi Road

Haidian District, Beijing, China 100193

Tel./fax: +86 10 62734195

E-mail address: sunying@cau.edu.cn (Y. Sun)

Abstract

This work reported a new method of design for the immobilization of acetylcholinesterase (AChE) based on its molecular structure to improve its sensitivity and stability. The immobilization binding site on the surface of AChE was determined using MOLCAD's multi-channel functionality. Then, 11 molecules ((+)-catechin, (-)-epicatechin, (-)-gallocatechin, hesperetin, naringenin, quercetin, taxifolin, (-)-epicatechin gallate, flupirtine, atropine, and hyoscyamine) were selected from the ZINC database (about 50000 molecules) as candidate affinity ligands for AChE. The fluorescence results showed that the binding constant K_b between AChE and the ligands ranged from 0.01344 $\times 10^4$ to 4.689 $\times 10^4$ M^{-1} and there was one independent class of binding site for the ligands on AChE. The AChE-ligand binding free energy ranged from -12.14 to -26.65 kJ mol^{-1}. Naringenin, hesperetin and quercetin were the three most potent immobilized affinity ligands. In addition, it was confirmed that the binding between the immobilized ligands only occurred at a single site, located in inactive area on the surface of AChE and did not affect the enzymatic activity as shown through a competition experiment and enzyme assay. This method based on protein-surface structural recognition with high sensitivity and stability can be used as a generic approach for design of the enzyme immobilization and biosensor development.

Key words: Acetylcholinesterase; Enzyme immobilization; Virtual screening; Protein-surface structural recognition; Enzyme activity.

Introduction

Acetylcholinesterase (AChE, EC 3.1.1.7) is a protein and also a type-B carboxylesterase enzyme with high catalytic activity located primarily in the synaptic cleft[1] and synthesized typically in nerve, muscle, and certain hematopoietic cells.[2] Its basic function is the hydrolytic metabolism of the neurotransmitter acetylcholine (ACh) into choline and acetate and work to terminate synaptic transmission in the nervous system.[3] Because it is the principal target enzyme inhibited by organophosphorus (OP) and carbamate (CB) compounds,[4-6] AChE has been used in biosensors as a biological recognition element for the detection of pesticides (e.g. malathion, paraoxon, trichlorfon, carbaryl) and nerve agents (e.g. soman, sarin, tabun, GF agent, VX).[7-10] The immobilization of this enzyme is the most crucial step in enzyme-based biosensor design and development. Immobilization can significantly improve the enzyme's performance especially storage stability and higher reproducibility compared with its free state.[11] Moreover, the biocatalytic activity of the immobilized enzyme directly determines the selectivity, sensitivity, and accuracy of the biosensors, hence why it has become a primary concern in biosensor design.

In the initial stage, Goodson, L. H et al., described that the first device of biosensors with immobilized cholinesterase appeared in 1976.[12] Since then, more and more AChE-based biosensors were developed.[13, 14] In recent years, thousands of reports about the design and development of the AChE-based biosensors were published as well as various immobilization methods and strategies including

adsorption, covalent attachment of the enzyme to silica, gold, carbon, polymers and nanomaterials (e.g. carbon nanotubes, graphene), entrapment in sol-gels and polymers, and cross-linking.[15-19] However, almost all the methods were difficult to control and usually yield randomly bound proteins. In other words, the orientation of the immobilized enzyme was irregular and ignored in its design. This can negatively affect enzyme conformation, limit enzyme activity, and lead to low biocatalytic efficiency.

The site-specific enzyme immobilization technique can increase the applicability and the stability of enzymes dramatically. Compared to the conventional methods of enzyme immobilization, site-specific enzyme immobilization effectively controls the orientation of immobilized enzymes and avoids reducing protein function by steric hindrance of available bioactive sites and reduction of protein stability.[20] Current methods for site-specific enzyme immobilization create (bio) affinity bonds between an activated support and a specific group of the protein sequence.[20, 21] Typically these methods rely on the affinity between the enzyme and specific molecules or groups (e.g. sugars, biotin, metal chelates, histidine or cysteine, azide moiety, peptides).[20-22] For AChE, the research of site-specific enzyme immobilization has only recently begun, and only a few papers about the methods of site-specific immobilization of AChE based on the overall structural characteristics (surface charge or hydrophobicity) have been reported.[22-25] Ivanov, Y et al., described how site-specific immobilization of AChE on chemically modified poly-(acrylonitrile-methyl-methacrylate-sodium vinylsulfonate) membranes could be used for the development of an amperometric biosensor. Other

papers have shown that the site-specific immobilization enzymes were used to detect a variety of pesticides.[23, 24] Ganesana, M. et al., reported that the site-specific affinity immobilization of(His)6-tagged AChE on Ni/NiO nanoparticles in the development of an electrochemical screen-printed biosensor could be used for the detection of paraoxon.[22] Chumphukam, O. et al., found a method of site-specific affinity immobilization AChE using a DNA aptamer that binds AChE with high affinity.[25] The main reason for the slow development is that few universal method has been designed for site-specific immobilization of the enzyme. Futhermore, the variance in different regions on the protein surface is often overlooked and the three-dimensional structural information of AChE was not used effectively in the design of enzyme immobilization.[26] Enzymes are (mostly) protein molecules in cells which work as catalysts.[27] Like all proteins, the structures of enzymes directly determine their biofunction especially catalytic activity and stability. Thus, in order to achieve the goal of site-specific immobilized AChE while maintaining activity and stability, the design of the immobilization method could be based on the structure of the enzyme. Like other previously researched enzymes, much of the research of AChE was focused on the active site's contribution to protein structure and function.[28-30] The inactive areas on the surface of enzyme were generally ignored. Fortunately, the three-dimensional structural information of AChE already elucidated through x-ray crystallographic techniques is sufficient to be used in protein surface analysis.[29]

Computational chemistry development, molecular modeling and structure-based

virtual screening (SBVS) have started to become widely applied in early-stage drug design. Because these techniques are based on the "lock and key" principle of ligand-target interaction, molecular docking have become the robust tools for design the site-specific enzyme immobilization of AChE. In this study, we combined molecular modeling, virtual screening, molecular docking, spectral experiments and enzyme assays to develop a new method of design for the immobilization of AChE based on protein-surface structural recognition. In order to reduce the negative effects of enzyme activity, the immobilization binding site located far away from the active site was found, evaluated and selected using MOLCAD's multi-channel functionality, a method used for structural analysis of molecular modeling. The next key step was the virtual screening of the functional immobilized affinity ligands by molecular docking. Finally, we reported the affinity and selectivity of the binding between AChE and immobilized affinity ligands using fluorescence methods and an enzyme assay.

Results and Discussion

Molecular modeling.

Acetylcholinesterase (AChE) was found to be a kind of globular protein[31] after its three-dimensional structure had been solved through x-ray crystallography. According to the amino acid sequence (**Figure 1b**), 583 residues made up AChE and four pieces of sequences were missing (unidentified) in the structural information in the PDB file (PDB ID:1F8U).[29] Two of them were in the middle (red) and the others (blue) were on

the head or at the tail end. Missing residues in the x-ray data of protein were very common, including those corresponding to particularly flexible regions of the protein. The missing loops (residues 259-264 and 493-494) in the middle of AChE sequence, located on the edge of the 3D model (**Figure 1a**), were very short, flexible and significantly affected its structural integrity, protein surface analysis and immobilization binding site discovery. The three-dimensional structures of the missing loops in the middle of AChE were fixed, optimized and evaluated based on the DOPE score by MODELLER[32] with default parameters. The results are shown in **Figure 1d and 1e**. Because of the little contribution to the results of this study, residues 1-4 and 544-583 were ignored.

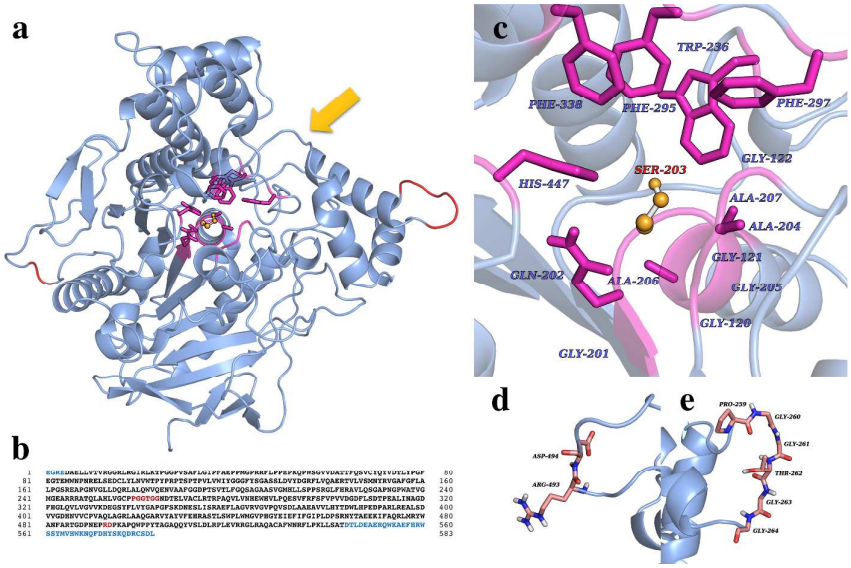

Figure 1 Three-dimensional structure of AChE. Panel (A) showed the ribbon model of acetylcholinesterase derived from x-ray crystallography (PDB: 1F8U); Red loop showed the missing loops by MODELLER; Magenta area showed the active site of

AChE; Yellow arrow indicated the location of AChE's substrate channel. Panel (B) showed the amino acidic sequences of AChE. Black, existing amino acid residues in 1F8U; Red, missing amino acid residues in the middle; Blue, missing amino acid residues at the beginning or the end. Panel (C) showed the structure of the active site of AChE. Panel (D) and (E) showed the structure of the missing loops, respectively. These illustrations were made with PyMOL on the basis of the atomic coordinates available at the Brookhaven Protein Data Bank (http://www.rcsb.org/pdb).

According to the x-ray crystal structure (PDB ID:1F8U) as shown in **Figure 1a** with a resolution of 2.9 Å, AChE is a single, non-glycosylated polypeptide chain of 539 amino acid residues that organizes to form a ball-shaped protein with the dimensions 151 Å × 151 Å × 247 Å. It also contains some water molecules. As shown in the **Figure 1c**, the activity site (magenta area), is in the center of protein and the Ser203, His447 are critical amino acid residues for the catalytic reaction.[33] From the report of AChE's inhibition mechanism, AChE's substrate channel (yellow arrow) is near Trp286 and Asp74 and is a peripheral site for inhibitor development.[33] Thus, to avoid affecting the conformation of these areas, it was crucial to maintain the enzymatic activity during use and the immobilization processes.

Immobilization binding site finding.

For site-specific immobilization (or directional immobilization) of AChE, a new

cavity on the surface of protein able to bind the functional ligands was needed. It was essential that the site was structurally stable, a certain size and far from the active site.

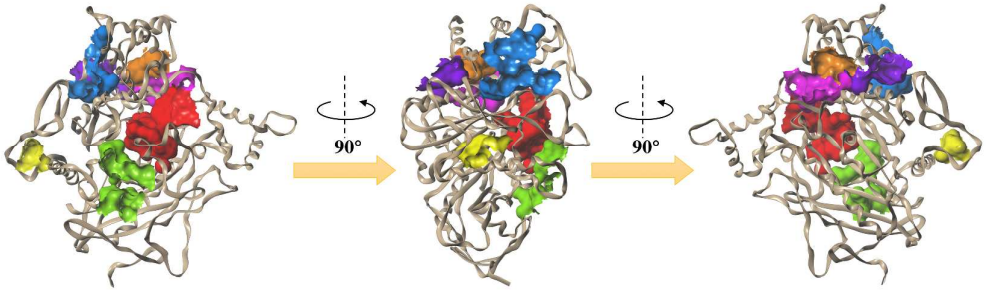

Figure 2 The cavities on the protein of AChE. The cavities included active site (red), Site1 (blue), Site2 (chartreuse), Site3 (magenta), Site4 (purple), Site5 (orange) and Site6 (yellow). These illustrations were made with Sybyl.

In total, six sites (**Figure 2 and Table S1**) were found on the surface of AChE, excluding the active site, using the Multi-Channel Surface[34] by SYBLE with the parameters Dot Density = 6.0 points/area, Probe Radius = 1.4 Å, Minimum Dots = 1000. They were distributed in different areas on the surface of AChE. Among them, Site2, Site3 and Site5 were very close to the active site or the substrate channel and thus had potentially negative effects on the catalytic activity of AChE. Because of its small size and instability, Site6 was excluded. Both Site1 and Site4 were far from the active site and of sufficient size (Volume > 350 $Å^3$). With its larger size, greater depth and higher stability, Site1 was chosen as the new immobilization site for site-specific immobilization of AChE.

After determining the immobilization site, its structural features and characteristics became the focus of attention. **Figure 3** includes the specific structural details of Site1 on the surface of AChE. The site is located in an interstice surrounded by a long α-helix and a β-sheet. The β-sheet acts like a strong wall that works to ensure the structural stability of Site1 as well as separate it from the active site. There is plenty of space in the pocket-like region for a small molecule. Moreover, a large number of polar amino acid residues are distributed in the cavity such as Arg525, Asp333, Ser399, Asp400, Asp404, Glu431, Arg521, Tyr510, etc. They are also potential hydrogen bond donors and receptors for ligand-AChE binding. Arginine and tyrosine residues are potential players in the π-π interaction of AChE with small molecule and help stabilize the conjugate structures of the ligands. All of these factors point to Site1 being a stable immobilization site and having a strong potential for the binding of a small molecule, especially those that utilize multiple hydrogen-bonding.

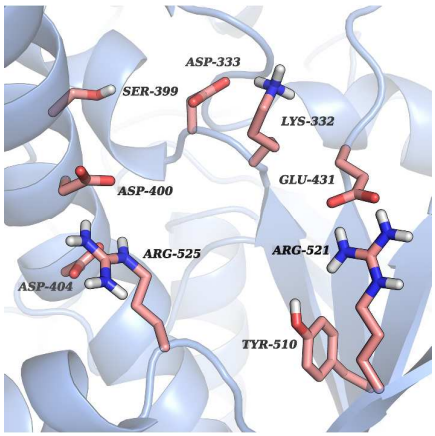

Figure 3 The structure of the immobilization site (Site1). The key amino acid

residues (Lys332, Asp333, Ser399, Asp400, Asp404, Glu431, Tyr510, Arg521, Arg525) in Site1 have been shown as a stick model and colored as per the atoms. This illustration was made with PyMOL.

Functional immobilized affinity ligand screening.

Functional immobilized affinity ligands are small molecules which were able to selectively bind to an inactive area (immobilization binding site) on a protein using structure-based virtual screening. In this research, the small molecule needed to have the following characteristics: (a) molecular weight between 50 and 550 Da (b) structural stability (c) purchasable (d) not very flexible. The files of molecules used to screen were from the ZINC database (http://zinc.docking.org/)[35] and in ready-to-dock. 54159 molecules were selected and composed into a small molecule library.

The functional immobilized affinity ligands screening using molecular docking by SYBLY had three stages: 1) initial screening 2) secondary screening 3) artificial selection.

The total score of the ligands was based on the Site1-ligand or activity site-ligand binding score of docking. The method of calculation was in the following: first, if the binding score was negative, zero was used in the calculation in place of the binding score. Second, the total score of ligands equaled Site1 binding score minus the activity site binding score.

In the initial screening, the parameters of high speed screening used in docking

were: Additional Starting Conformations per Molecule = 5; Max Conformations per Fragment = 20; Density of Search = 6.00 in spin alignment method; Maximum Number of Poses per Ligand = 20; Minimum RMSD Between Final Poses = 0.50; others were set to default. After this screening, and the 200 molecules with the highest score were used in the next step as the new molecular library.

In the secondary screening, the parameters of the high quality screen used in docking were: Additional Starting Conformations per Molecule = 10; Max Conformations per Fragment = 50; Density of Search = 9.00 in spin alignment method; Maximum Number of Poses per Ligand = 100; Minimum RMSD Between Final Poses = 0.05; calculated the CScore; others were set to the default. The total score of each ligand was then calculated.

In the artificial selection step, the functional immobilized affinity ligands were selected based on the total score of the ligands, CScore of Site1-ligands, the conformation of binding, and the structural features of the ligands. Some molecules that were too flexible, had an abnormal conformation, or located on the edge of the pocket, were excluded. Although a certain degree of randomness existed in the artificial selection, it removed a vast majority of the results with noticeable error.

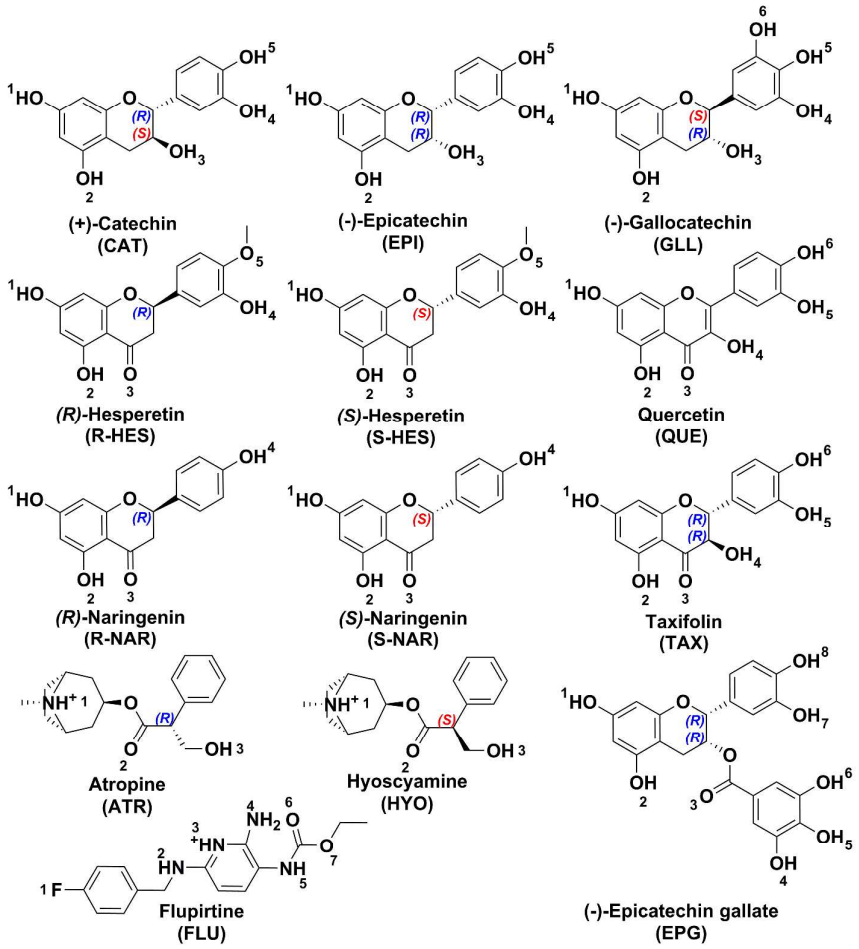

Figure 4 Molecular structure of ligands. The parts of chiral atoms of ligands were marked.

13 ligands were selected using the above method, and their structures and abbreviations were shown in **Figure 4**. There were three kinds of compounds: flavonoids, anticholinergic drugs, and aminopyridine drugs. The flavonoids included (+)-catechin, (-)-epicatechin, (-)-gallocatechin, (*R*)-hesperetin, (*S*)-hesperetin, (*R*)-naringenin, (*S*)-naringenin, quercetin, taxifolin and (-)-epicatechin gallate. The anticholinergic drugs included atropine and hyoscyamine. The aminopyridine drugs

included flupirtine. In pH neutral environments, atropine, hyoscyamine and flupirtine were singly-positively charged, and the others were uncharged. In addition, there were four pairs of enantiomers, which were atropine and hyoscyamine, (+)-catechin and (-)-epicatechin, (*R*)-hesperetin and (*S*)-hesperetin, (*R*)-naringenin and (*S*)-naringenin.

Fluorescence of the AChE-ligand complex.

Fluorescence measurement is a simple and non-destructive method used to explore the binding between proteins (such as lysozyme,[36] serum albumin,[37] hemoglobin,[38] etc.) and ligands. The variation of different fluorescence spectroscopic characteristics (such as fluorescence intensity, shapes, etc.) is extensively optimized for the ligand's probing hydrophobicity or polarity, selective binding to one of their protonation states, subunit association, protein conformational changes, and so on.[39] The amino acids phenylalanine, tryptophan and tyrosine,[40] as fluorescence probes around protein, are usually used to estimate the binding affinity of the ligands in the complexes and to detect conformational changes. Thus, in order to determine the results of the functional immobilized affinity ligands screening, fluorescence experiments of AChE with 11 ligands (hesperetin and naringenin using the racemate) were carried out. The interaction of the ligands with AChE and the conformational changes in AChE were studied by measuring the intrinsic protein fluorescence intensity before and after the addition of the ligand. **Figure S1** shows the fluorescence emission spectra of AChE in the absence and presence of the ligands with an emission peak at 330 nm by the

excitation at 280nm. The fluorescence intensity was gradually decreased along with an increase in the ligands' concentrations which caused slight shifts of part of the complex spectra towards longer wavelengths. These phenomena implied that the binding of ligands to AChE quenched the intrinsic fluorescence of the protein and the AChE-ligand complex was produced. Moreover, the bathochromic shift (< 8 nm) of the maximum emission wavelength revealed that the microenvironment around the binding site was altered, and there was a higher hydrophilicity in the binding site region.[41] Taking into account the structures of the ligands as well as their polar and hydrophilic characteristics, multiple hydrogen bonds were formed between the AChE and ligand in the binding process. This increased the hydrophilicity of the region near Site1, which caused the bathochromic shift.

Fluorescence quenching is the decrease of the quantum yield of fluorescence from a fluorophore which is induced by a variety of molecular interactions with a quencher molecule. This mechanism is similar to that of the AChE-ligand interaction. Fluorescence quenching can be dynamic, resulting from collisional encounters between the fluorophore and the quencher, or static, resulting from the formation of a ground state complex between the fluorophore and the quencher. Fluorescence quenching is described by the Stern-Volmer equation:[40]

$$\frac{F_0}{F} = 1 + k_q \tau_0 [Q] = 1 + K_{SV}[Q] \qquad \textbf{Equation (1)}$$

where F_0 and F are the fluorescence intensities before and after the addition of the quencher, respectively, k_q is the bimolecular quenching constant, τ_0 is the lifetime of the

fluorophore in the absence of the quencher (the fluorescence lifetime of the biopolymer is 10^{-8} s), [Q] is the concentration of the quencher, and K_{SV} is the Stern–Volmer quenching constant. Eq. (1) was used to determine K_{SV} by the linear regression of a plot of F_0/F against [Q].

The quenching data was analyzed according to the Stern-Volmer equation **Eq. (1)**, and the corresponding results fitted from Stern-Volmer plots **Figure S2** are summarized in **Table 1**. The results visibly show that the range of Stern-Volmer quenching constant(K_{SV}) was 0.08333 $\times 10^4$ M^{-1} to 5.534 $\times 10^4$ M^{-1}. Meanwhile, the value of k_q was very close (ATR and HYO) or higher than the maximum value for diffusion-controlled quenching in water ($\sim 10^{10}$ $M^{-1}s^{-1}$),[40] indicating that the result is typically the dissociation of weakly bound complexes. As a result, there is smaller amounts of static quenching. This means the ligands were able to bind to AChE and the presence of AChE-ligand complexes were confirmed.

Table 1 Stern-Volmer quenching constants (K_{SV}), bimolecular quenching constants (k_q), affinity (K_b), the number of molecules (n) and binding free energy (ΔG) for the molecular recognition of AChE with ligands.

Compounds	AChE-ligand							AChE-TAC-ligand			AChE-GAL-ligand		
	K_{SV} ($\times 10^4$ M^{-1})	k_q ($\times 10^{12}$ $M^{-1}s^{-1}$)	R^a	K_b ($\times 10^4$ M^{-1})	n	ΔG (kJ mol^{-1})	R^a	K_{SV} ($\times 10^4$ M^{-1})	k_q ($\times 10^{12}$ $M^{-1}s^{-1}$)	R^a	K_{SV} ($\times 10^4$ M^{-1})	k_q ($\times 10^{12}$ $M^{-1}s^{-1}$)	R^a
CAT	2.670	2.670	0.9987	0.3173	0.80	-19.98	0.9995	2.621	2.621	0.9969	2.594	2.594	0.9972
EPI	1.834	1.834	0.9995	0.3138	0.84	-19.95	0.9993	1.825	1.825	0.9991	1.886	1.886	0.9988
GLL	0.9260	0.9260	0.9978	0.1340	0.82	-17.84	0.9995	0.9324	0.9324	0.9972	0.9138	0.9138	0.9973
HES	5.534	5.534	0.9994	3.676	0.96	-26.04	0.9995	5.393	5.393	0.9991	5.428	5.428	0.9988
NAR	4.420	4.420	0.9998	4.689	1.00	-26.65	0.9997	4.385	4.385	0.9995	4.293	4.293	0.9994
QUE	5.444	5.444	0.9997	2.048	0.91	-24.60	0.9988	5.386	5.386	0.9995	5.372	5.372	0.9996
TAX	2.642	2.642	0.9988	0.4069	0.83	-20.59	0.9991	2.579	2.579	0.9991	2.596	2.596	0.9986
EPG	3.542	3.542	0.9996	0.4350	0.81	-20.76	0.9986	3.581	3.581	0.9989	3.439	3.439	0.9991
FLU	1.905	1.905	0.9981	0.3057	0.83	-19.88	0.9987	1.915	1.915	0.9983	1.889	1.889	0.9986
ATR	0.09968	0.09968	0.9984	0.01377	0.76	-12.20	0.9998	0.09711	0.09711	0.9979	0.09664	0.09664	0.9978
HYO	0.08333	0.08333	0.9974	0.01344	0.78	-12.14	0.9995	0.08153	0.08153	0.9976	0.08405	0.08405	0.9971

[a] R is the correlation coefficient.

Binding location

The binding location of immobilized affinity ligands is just as important as the binding ability of these ligands. This is because location is directly related to the characteristics and performance of the immobilized enzyme. Therefore, in order to further identify immobilization binding sites on AChE, site marker competition experiments were conducted by using drugs that specifically bound to the active site on AChE. Based on the enzyme assay and crystallographic analyses of AChE,[42] the acetylcholinesterase (AChE) inhibitors tacrine[43] (TAC) and galantamine[44] (GAL) were chosen because they selectively bind to the active site of AChE and efficiently inhibit enzyme activity. The inhibitory constants (K_i) of tacrine and galantamine are 3.57 nM and 6.19 nM,[42] respectively, indicating that they preferentially bind to the active site and completely prevent other molecules, even the substrate, from binding to the active site of AChE. The fluorescence intensity data of the AChE–immobilized ligands system with the presence of active site markers was analyzed using **Eq. (1)**, and the corresponding values of K_{SV} are listed in **Table 1**. The association constant did not remarkably increase or decrease after the addition of tacrine or galantamine which had a difference of less than 4%. These results are evidence that the binding between AChE and immobilized affinity ligand does not occur in or near the active site, including the substrate channel. It also showed that the inhibition of the active site did not affect binding to the immobilization binding site.

An enzyme activity assay of AChE was performed for a more intuitive and direct

assessment of the effect of ligand binding on the enzyme. As shown in **Figure S3**, the results supported that the enzyme activity of AChE had not changed significantly at the 0.05 level (P 0.05) in the binding process, even with a 10-fold excess of ligand. This exciting result for AChE immobilization were combined with competitive experiment and was also consistent with molecular docking. This meant that the immobilization binding site and active site of AChE were independent of each other, consistent with the original goals and design of this project.

Binding affinity

To characterize the binding properties of the ligands with AChE, the relationship between fluorescence quenching intensity and the concentration of the quencher was determined. The binding constant (K_b) and binding affinity (n) was calculated using the equation for static quenching process:[45]

$$\log\frac{F_0 - F}{F} = \log K_b + n\log[Q] \qquad \textbf{Equation (2)}$$

In this equation, F_0 and F are the fluorescence intensities in the absence and presence of quencher, respectively, K_b is the association constant, n is the number of molecules that interact simultaneously with each site of the protein, and [Q] is the concentration of quencher. A plot of $\log(F_0 - F)/F$ against $\log[Q]$ can be used to calculate K and n.

The binding free energy (ΔG_{bind}) was calculated using the equation:

$$\Delta G_{bind} = -RT\ln K_b \qquad \textbf{Equation (3)}$$

where R and T are the gas constant and temperature, respectively.

The plot of log $[(F_0 - F)/F]$ versus log [Q] for the AChE-ligand complex showed a straight line (**Figure S4**) and the values of binding constant (K_b) and the binding affinity (n) obtained were as shown in **Table 1**. The value of n was approximately equal to 1, which implied that there was one independent class of binding site for the ligands on AChE. This was consistent with the results of the spectral experiment enzyme assay.

In general, the results of binding affinity showed that all the ligands selected from molecular screening demonstrated a certain binding affinity to AChE and the values differed between each other. Based on their affinities to AChE, the ligands were categorized into three levels: the first was high-affinity ($K_d > 10^4$ M^{-1}), which included naringenin, hesperetin and quercetin; the second was medium-affinity ($10^3 < K_d \leq 10^4$ M^{-1}), which included (+)-catechin, (-)-epicatechin, (-)-gallocatechin, taxifolin, (-)-epicatechin gallate and flupirtine; and the third was low-affinity ($10^2 < K_d \leq 10^3$ M^{-1}), which included atropine and hyoscyamine.

To develop a better analysis of the results and understand the mechanism of the relationship between the complex structure and binding affinity, the binding poses by docking shown in **Figure 5** were determined. These are the conformation of the interaction between Site1 and each ligand. The results, including the detail of hydrogen bonding analysis, are listed in **Table 2**.

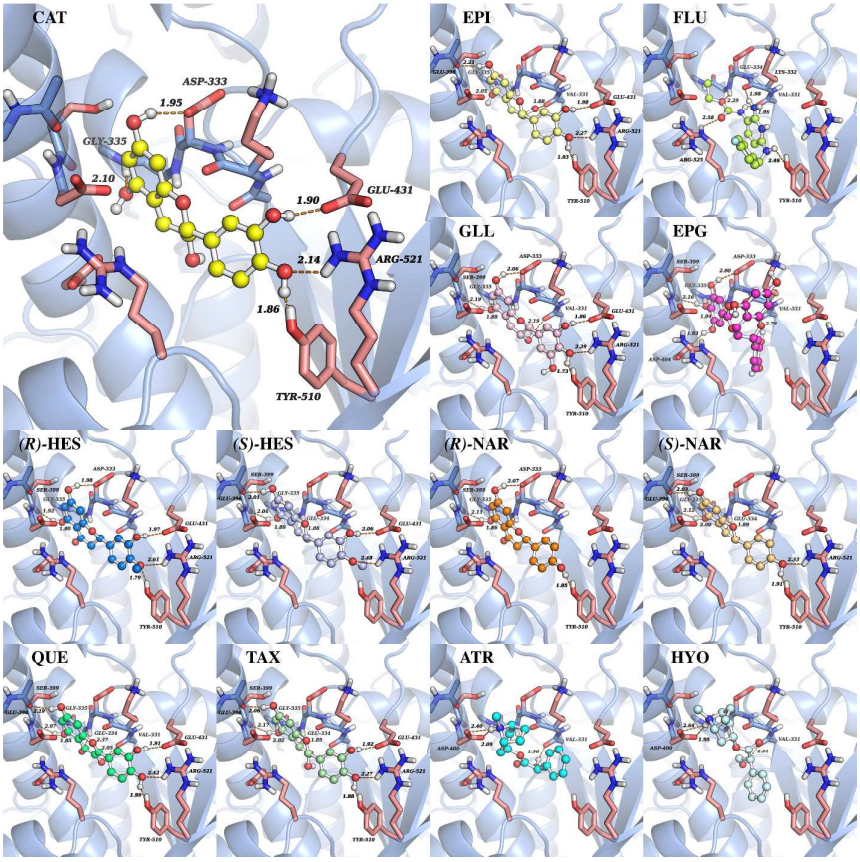

Figure 5 Molecular modeling of ligands docked to AChE. The critical amino acid residues around (+)-catechin (yellow), (-)-epicatechin (pale yellow), (-)-gallocatechin (light pink), epicatechin gallate (light magenta), (*R*)-hesperetin (marine), (*S*)-hesperetin (light blue), (*R*)-naringenin (orange), (*S*)-naringenin (light orange), quercetin (lime green), taxifolin (pale green), atropine (cyan), hyoscyamine (pale cyan) and (-)-flupirtine (limon) have been manifested in stick model form, respectively. These illustrations were made with PyMOL.

Table 2 Hydrogen bond analyses from the results of molecular modeling for AChE with ligands.

Compounds	Protein	Ligands	Distance(Å)

CAT	ASP-333: -*COO*	-*OH* (1)	1.95
	GLY-335: -*NH* (mainchain)	-*OH* (2)	2.10
	GLU-431: -*COO*	-*OH* (4)	1.90
	ARG-521: -NH_2	-*OH* (5)	2.14
	TYR-510: -*OH*	-*OH* (5)	1.86
EPI	GLU-396: -*CO* (mainchain)	-*OH* (1)	2.21
	GLY-335: -*NH* (mainchain)	-*OH* (2)	2.05
	VAL-331: -*CO* (mainchain)	-*OH* (3)	1.88
	GLU-431: -*COO*	-*OH* (4)	1.98
	ARG-521: -NH_2	-*OH* (5)	2.27
	TYR-510: -*OH*	-*OH* (5)	1.93
GLL	ASP-333: -*COO*	-*OH* (1)	2.06
	GLY-335: -*NH* (mainchain)	-*OH* (2)	1.88
	SER-399: -*CO* (mainchain)	-*OH* (2)	2.19
	VAL-331: -*CO* (mainchain)	-*OH* (3)	2.19
	ARG-521: -NH_2	-*OH* (5)	2.29
	TYR-510: -*OH*	-*OH* (5)	1.73
	GLU-431: -*COO*	-*OH* (6)	1.86
(R)-HES	ASP-333: -*COO*	-*OH* (1)	1.98
	GLY-335: -*NH* (mainchain)	-*OH* (2)	1.80
	SER-399: -*CO* (mainchain)	-*OH* (2)	1.92
	GLU-431: -*COO*	-*OH* (4)	1.97
	ARG-521: -NH_2	-*O*- (5)	2.61
	TYR-510: -*OH*	-*O*- (5)	1.70
(S)-HES	GLU-396: -*CO* (mainchain)	-*OH* (1)	2.01
	GLY-335: -*NH* (mainchain)	-*OH* (2)	1.89
	SER-399: -*CO* (mainchain)	-*OH* (2)	2.06
	GLU-334: -*NH* (mainchain)	-*CO* (3)	1.88
	GLU-431: -*COO*	-*OH* (4)	2.06
	ARG-521: -NH_2	-*O*- (5)	2.48
(R)-NAR	ASP-333: -*COO*	-*OH* (1)	2.07
	GLY-335: -*NH* (mainchain)	-*OH* (2)	1.86
	SER-399: -*CO* (mainchain)	-*OH* (2)	2.11
	TYR-510: -*OH*	-*OH* (4)	1.85
(S)-NAR	GLU-396: -*CO* (mainchain)	-*OH* (1)	2.03
	GLY-335: -*NH* (mainchain)	-*OH* (2)	2.00
	SER-399: -*CO* (mainchain)	-*OH* (2)	2.12
	GLU-334: -*NH* (mainchain)	-*CO* (3)	1.89
	ARG-521: -NH_2	-*OH* (4)	2.33
	TYR-510: -*OH*	-*OH* (4)	1.91

QUE	GLU-396: -*CO* (mainchain)	-*OH* (1)	2.19
	GLY-335: -*NH* (mainchain)	-*OH* (2)	1.85
	SER-399: -*CO* (mainchain)	-*OH* (2)	2.07
	GLU-334: -*NH* (mainchain)	-*CO* (3)	2.37
	VAL-331: -*CO* (mainchain)	-*OH* (4)	2.05
	GLU-431: -*COO*	-*OH* (5)	1.91
	ARG-521: -NH_2	-*OH* (6)	2.42
	TYR-510: -*OH*	-*OH* (6)	1.99
TAX	GLU-396: -*CO* (mainchain)	-*OH* (1)	2.06
	GLY-335: -*NH* (mainchain)	-*OH* (2)	2.02
	SER-399: -*CO* (mainchain)	-*OH* (2)	2.17
	GLU-334: -*NH* (mainchain)	-*CO* (3)	1.85
	GLU-431: -*COO*	-*OH* (5)	1.92
	ARG-521: -NH_2	-*OH* (6)	2.27
	TYR-510: -*OH*	-*OH* (6)	1.88
EPG	ASP-333: -*COO*	-*OH* (4)	2.00
	GLY-335: -*NH* (mainchain)	-*OH* (5)	1.94
	SER-399: -*CO* (mainchain)	-*OH* (5)	2.16
	ASP-404: -*COO*	-*OH* (6)	1.93
	VAL-331: -*CO* (mainchain)	-*OH* (7)	2.76
FLU	TYR-510: -*OH*	-*NH* (2)	2.46
	LYS-332: -*CO* (mainchain)	-NH_2 (4)	1.98
	VAL-331: -*CO* (mainchain)	-*NH* (5)	1.96
	ARG-525: -NH_2	-*CO* (6)	2.58
	GLU-334: -*NH* (mainchain)	-*O*- (7)	2.29
ATR	ASP-400: -*COO*	-*NH* (1)	2.09
	ASP-400: -*COO*	-*NH* (1)	2.40
	VAL-331: -*CO* (mainchain)	-*OH* (3)	1.98
HYO	ASP-400: -*COO*	-*NH* (1)	1.95
	ASP-400: -*COO*	-*NH* (1)	2.64
	VAL-331: -*CO* (mainchain)	-*OH* (3)	2.01

The results have also shown that the ligands were “lying down” in the Site1 pocket and the different kinds of ligands had different binding characteristics with AChE. Flavonoids and flupirtine had a relatively high affinity to AChE because there have several hydrogen bonds between themselves and the polar residues in Site1 of

AChE. The binding affinities of the ligands belonging to anticholinergic drugs were significantly lower than the others. This is because atropine and hyoscyamine have a lack of hydrogen bond donors or acceptors which prevented the ligands from entering deeper into the binding site. More in-depth analysis of binding for each type of molecule is detailed below.

Flavonoids: These molecules had an extraordinarily similar parent structure, except (-)-epicatechin gallate which had an extra gallic acid group. The main structural difference between them was the number and location of the hydroxyl (-*OH*) and carbonyl (-*CO*) groups. All of their binding affinities to AChE ranged from high to medium, but their binding profiles were generally similar. The multiple hydrogen bonds between ligands and Site1 at different regions were another main factor in the stability of the complex. More specifically, Glu431, Tyr510 and Arg521, which are located on edge of the pocket, interact with the phenolic hydroxyl groups and the oxygen atom of phenyl ester on the single benzene ring of ligands. These interactions stabilize one side of the molecule. Asp333 and the main chain of Glu334, Gly335, Glu396, Ser399, which are located in the pocket, interact with the phenolic hydroxyl groups on the fused ring of the ligands, stabilizing the other side of the molecule. Together, these multiple hydrogen bonds fix the molecules firmly in the pocket. However, the most critical characteristic of the flavonoids is their flake-like shape, excluding (-)-epicatechin gallate. This helps the ligands enter deeper into the binding site and reduces the effect of the crash with Site1. If the flexibility of guanidinium

group on arginine is taken into consideration, there is a great possibility that there is a π-π interaction between Arg525, which is parallel to the fused ring of flavonoids, and the π-conjugated ring on the flavonoid ligands. Because of these reasons, flavonoid molecules are able to selectively bind to Site1 with great binding strength.

The ranking of binding affinities of all the flavonoids from highest to lowest is NAR > HES > QUE >> EPG, TAX > CAT, EPI >GLL. The major factors that affect the binding affinities were the influence of steric hindrance on conformation properties and the molecular structure of the ligands. Looking first at naringenin and hesperetin, these molecules do not have hydroxyl groups (not including the phenolic hydroxyl groups) on their fused ring. This meant that these ligands entered the binding site more easily and deeply, while conforming to the shape of Site1. Although quercetin has these hydroxyl groups in its fused ring, its fully π-conjugated system allows all its atoms to lie almost in the same plane, and so steric hindrance was significantly reduced. The binding affinity of (-)-gallocatechin was the lowest among the flavonoids and has three hydroxyl groups on its single benzene ring. Naringenin had the highest binding affinity and only has a single phenolic hydroxyl group on its single benzene ring. It could be inferred that the number of functional groups on the single benzene ring of flavonoids directly affects the steric hindrance of the AChE-ligands binding process and excessive groups negatively affect their binding affinity.

Aminopyridine drugs: Flupirtine is a linear molecule based on its conjugated structure, which is beneficial for entering deeply into Site1 as well as for binding.

Flupirtine is also rich in polar group which act as hydrogen bond acceptor and donors. This is important as it makes five hydrogen bonds with AChE. More importantly, the positive charge on the conjugate groups of this ligand increases the electrostatic attraction between it and AChE. Overall, the binding affinity between flupirtine and AChE is medium in intensity.

Anticholinergic drugs: Atropine and hyoscyamine bind to AChE extraordinarily similarly. They both bind through an interaction between the Asp400 on Site1 and the nitrogen atom of a tertiary amine, which is a strong double interaction. This double hydrogen bond system is between the carboxyl group of Asp400 and the hydrogen atoms connected to the nitrogen on atropine or hyoscyamine. In pH neutral environments, the carboxyl group of Asp400 has a negative charge and the nitrogen on atropine has a positive charge, indicating that this is an electrostatic interaction. A hydrogen bond between Val333 on the mainchain and hydroxyl group (-*OH*) on the ligands further fix these molecules to the binding site. Because of the lack of hydrogen bond acceptors or donors, part of the benzene ring on the ligands is located outside the pocket and is not conducive to the stability of the complex. All of the results indicate that atropine and hyoscyamine are able to selectively bind to the immobilization site with moderate intensity. This conclusion was proved in the spectral experiment and in their binding affinities (0.01377 - 0.01344 $\times 10^4$ M^{-1}) which were lower than other ligands' (flavonoids and flupirtine). Traditionally, atropine and hyoscyamine as anticholinergic drugs were thought to act on the muscarinic acetylcholine receptor. In

1970, Kato, G. et al., reported that there were at least two distinguishable binding sites (a catalytic site and an unknown anionic site) in AChE and used NMR to determine that atropine was able to bind to the inactive site.[46] Our work could help elucidate this pharmacological mechanism.

Overall, these results showcased that the ligands selected from molecular virtual screening were able to selectively bind to the immobilization site of AChE and their complexes were firm and stable. The immobilized binding did not cause adverse effects to the biocatalytic activity of AChE and the details of the binding mechanism were revealed. The immobilized affinity ligands, especially naringenin, hesperetin and quercetin, can be used for development of AChE-based biosensors in future research. Considering immobilization mechanisms, although the binding location has not been sufficiently and completely confirmed based on the existing data, the binding affinity order obtained from fluorescence experiment between each ligand and Site1 can be explained by the binding structural characteristics. Thus it is extremely possible that the binding of immobilized ligands occurs on Site1. This project also showed how research on the inactive areas of a protein's surface is a potential source for valuable information not limited to enzyme immobilization and is worthy of further in-depth studies.

Conclusions

In this work, we proposed a new method for the site-specific immobilization of AChE based on protein surface structure analysis and functional immobilized affinity ligand design using molecular modeling, virtual screening and spectroscopic techniques. The immobilization binding site (Site1) on the surface of AChE was determined and 11 molecules were selected as functional immobilized affinity ligands. Fluorescence experimental results demonstrate that the binding between the immobilized ligands and AChE had adequate affinity and selectivity for enzyme immobilization, especially naringenin, hesperetin and quercetin. Moreover, the binding between the immobilized ligands and AChE did not affect the enzymatic activity of AChE, and there was one independent class of binding site for the ligands on AChE. This new method of enzyme immobilization offers a novel insight into the immobilization of the protein, which could be used as a preliminary method for biosensor design. These results could open the door to new avenues in enzyme immobilization and offer useful tools for the field of enzyme technology and biocatalysis.

Materials and Methods

Materials

Acetylcholinesterase (EC 3.1.1.7, lyophilized powder), (+)-catechin hydrate (≥98%), (-)-epicatechin (≥90%), (-)-gallocatechin (≥98%), (±)-hesperetin (≥95%), (±)-naringenin (≥95%), quercetin (≥95%), taxifolin (≥99%) and tacrine hydrochloride

hydrate (≥99%) were purchased from Sigma-Aldrich Trading Co., Ltd. (Shanghai, China) and used without further purification. Atropine sulfate monohydrate (≥98.5%), (-)-epicatechin gallate (≥99%), flupirtine maleate salt (≥97%), hyoscyamine hydrobromide (≥98%) and galantamine hydrobromide (≥98%) were purchased from the J&K Scientific Ltd. (Beijing, China) and used without further purification. Deionized water was generated by a Milli-Q Ultrapure Water Purification Systems from Millipore (Billerica, MA) and all the experiments were performed in 0.05 mol L^{-1} Tris -HCl buffer of pH = 7.4 containing 0.15 mol L^{-1} NaCl except where specified. The pH was checked with a FE20K-Plus pH meter (Mettler Toledo, China). Dilutions of the AChE (500μg/ml) stock solution in Tris-HCl buffer were prepared immediately before use and the concentration of AChE was determined spectrophotometrically using $E_{1cm}^{1\%}$ of 18.0 at 280nm.[47] All other reagents utilized were of analytical grade and received from Sigma-Aldrich.

Methods

Molecular modeling

Molecular modeling of AChE was carried out on a Linux workstation. The crystal structure of AChE (PDB ID: 1F8U at 2.9 Å resolution, chain A) was taken from the Brookhaven Protein Data Bank (http://www.rcsb.org/pdb/). Hydrogen atoms were computationally added using the H++ web server (http://biophysics.cs.vt.edu/H++/)[48] with AMBER parm99 force-field. The missing loops were built by using MODELLER (version 9.15, https://salilab.org/modeller/)[32] with default parameters. Molecular

modeling of AChE and visualization of the models were conducted with PyMOL (version 1.8.7.0, http://www.pymol.org/) on Linux workstation.

Binding site finding and molecular virtual screening

Immobilization binding sites were found with MOLCAD's multi-channel functionality by SYBYL (version 7.3, http://tripos.com/)[49] on a Linux workstation with the parameters Dot Density = 6.0 points/area, Probe Radius = 1.4 Å, Minimum Dots = 1000. Visualization of its result was rendered using Sybyl. The three-dimensional structures of the ligands with their molecular electronic structure were downloaded from the ZINC database (http://zinc.docking.org/)[35] and the initial structure of the molecule was produced using Sybyl. The Surflex-Dock program,[49] which employs an automatic flexible docking algorithm, was used to calculate the possible conformations of the ligand binding to AChE. Finally, the visualization of the molecular docking results was done with the PyMOL program.

Steady state fluorescence measurements

Fluorescence measurements were executed with a F-7000 spectrofluorimeter (Hitachi, Japan) equipped with a 1.0cm quartz cell and a thermostatic bath (LAUDA Alpha RA12) set to 298 K. The excitation and emission slits were set at 2.5 nm each, intrinsic fluorescence was carried out by exciting the stirred protein solution at 280 nm, and the emission spectra were recorded in the wavelength range of 290-500 nm at a

scanning speed of 240 nm min^{-1}.

Competition experiment

Binding location studies between AChE and the ligands in the presence of two typical active site markers (tacrine and galantamine) were performed using the fluorescence titration approach. The concentrations of AChE and active site markers were equimolar (2.0 μmol L^{-1}), and the immobilized affinity ligand was added to the AChE-site marker mixtures. An excitation wavelength of 280 nm was chosen, and the fluorescence emission wavelength set from 290 to 500 nm.

Enzyme assay

The AChE (EC 3.1.1.7) activity was determined using a method described by Ellman et al., AChE and the ligand was added to 3mL of reaction buffer (prepared by mixing 2.95mL of phosphate buffer 0.050 mol L^{-1} at pH 8.0 and 50μL of acetylthiocholine chloride 0.050 mol L^{-1}).[50] After a 5 mins incubation at 37°C, 1.0mL of sodium dodecyl sulfate (SDS) 10 g L^{-1} solution was added and mixed. Then, 50μL of reagent 5,5-dithiobis-2-nitrobenzoic acid (DTNB) 0.022 mol L^{-1} solution was added and the measurements carried out using a Lambda-25 double-beam spectrophotometer (Perkin-Elmer, USA) at 412 nm. The reaction solution was used as a blank.

Acknowledgements

This work was financially supported by the National Natural Science Foundation of China (Nos. 31171693 and 31471652). We thank Rory Vu Mather who is studying at Washington University in St.Louis for his linguistic assistance during the preparation of this manuscript.

Conflict of Interest Statement

The authors declare no competing financial interest.

Supporting Information description

The result of immobilization binding site finding, steady state fluorescence of AChE with various amounts of each ligand, Stern-Volmer plot describing fluorescence quenching of AChE, enzyme activity of AChE with ligands, and the plots of log $[(F_0 - F)/F]$ versus log $[Q]$ for the AChE-ligand system.

Abbreviations

AChE, acetylcholinesterase; CAT, (+)-catechin; EPI, (-)-epicatechin; GLL, (-)-gallocatechin; HES, hesperetin; NAR, naringenin; QUE, quercetin; TAX, taxifolin; EPG, (-)-epicatechin gallate; FLU, flupirtine; ATR, atropine; HYO, hyoscyamine; Tris, tris(hydroxymethyl)aminomethane; Ala, alanine; Arg, arginine; Asp, aspartic acid; Gln, glutamine; Glu, glutamic acid; Gly, glycine; His, histidine; Lys, lysine; Phe, phenylalanine; Ser, serine; Trp, tryptophan; Tyr, tyrosine; Val, valine

Reference

(1) Bittner, E. A., and Martyn, J. A. J. (2013) Chapter 18 - Neuromuscular Physiology and Pharmacology A2 - Hemmings, Hugh C, *Pharmacology and Physiology for Anesthesia*. (Egan, T. D., Ed.) pp 309-324, Chapter 18, W.B. Saunders, Philadelphia.

(2) Taylor, P., Camp, S., and Radić, Z. (2009) Acetylcholinesterase A2 - Squire, Larry R, *Encyclopedia of Neuroscience* pp 5-7, Chapter 2, Academic Press, Oxford.

(3) English, B. A., and Webster, A. A. (2012) Chapter 132 - Acetylcholinesterase and its Inhibitors, *Primer on the Autonomic Nervous System*. (Biaggioni, I., Burnstock, G., Low, P. A., and Paton, J. F. R., Eds.) pp 631-633, Chapter 132, Academic Press, San Diego.

(4) Liao, S., Han, W., Ding, H., Xie, D., Tan, H., Yang, S., Wu, Z., Shen, G., and Yu, R. (2013) Modulated Dye Retention for the Signal-On Fluorometric Determination of Acetylcholinesterase Inhibitor. *Anal. Chem. 85*, 4968-4973.

(5) Mileson, B. E., Chambers, J. E., Chen, W. L., Dettbarn, W., Ehrich, M., Eldefrawi, A. T., Gaylor, D. W., Hamernik, K., Hodgson, E., Karczmar, A. G., et al. (1998) Common Mechanism of Toxicity: A Case Study of Organophosphorus Pesticides. *Toxicol. Sci. 41*, 8-20.

(6) Marrs, T. C. (1993) Organophosphate poisoning. *Pharmacol. Ther. 58*, 51-66.

(7) Dzudzevic Cancar, H., Soylemez, S., Akpinar, Y., Kesik, M., Göker, S., Gunbas, G., Volkan, M., and Toppare, L. (2016) A Novel Acetylcholinesterase Biosensor: Core–Shell Magnetic Nanoparticles Incorporating a Conjugated Polymer for the Detection of Organophosphorus Pesticides. *ACS Appl. Mater. Interfaces 8*, 8058-8067.

(8) Liu, D., Chen, W., Wei, J., Li, X., Wang, Z., and Jiang, X. (2012) A Highly Sensitive, Dual-Readout Assay Based on Gold Nanoparticles for Organophosphorus and Carbamate Pesticides. *Anal. Chem. 84*, 4185-4191.

(9) Liu, X., Song, M., Hou, T., and Li, F. (2017) Label-Free Homogeneous Electroanalytical Platform for Pesticide Detection Based on Acetylcholinesterase-Mediated DNA Conformational Switch Integrated with Rolling Circle Amplification. *ACS Sens. 2*, 562-568.

(10) Onder, S., Schopfer, L. M., Cashman, J. R., Tacal, O., Johnson, R. C., Blake, T. A., and Lockridge, O. (2018) Use of Hupresin to capture red blood cell acetylcholinesterase for detection of soman exposure. *Anal. Chem. 90*, 974-979.

(11) Sassolas, A., Blum, L. J., and Leca-Bouvier, B. D. (2012) Immobilization strategies to develop enzymatic biosensors. *Biotechnol. Adv. 30*, 489-511.

(12) Goodson, L. H., and Jacobs, W. B. (1976) [43] Monitoring of air and water for enzyme inhibitors, *Methods in Enzymology* pp 647-658, Chapter 43, Academic Press.

(13) Skládal, P. (1996) Biosensors Based on Cholinesterase for Detection of Pesticides. *Food Technol. Biotechnol. 34*, 43-49.

(14) Schulze, H., Vorlová, S., Villatte, F., Bachmann, T. T., and Schmid, R. D. (2003) Design of acetylcholinesterases for biosensor applications. *Biosens. Bioelectron. 18*, 201-209.

(15) Andreescu, S., and Marty, J.-L. (2006) Twenty years research in cholinesterase biosensors: From basic research to practical applications. *Biomol. Eng. 23*, 1-15.

(16) Van Dyk, J. S., and Pletschke, B. (2011) Review on the use of enzymes for the detection of organochlorine, organophosphate and carbamate pesticides in the environment. *Chemosphere 82*, 291-307.

(17) Pundir, C. S., and Chauhan, N. (2012) Acetylcholinesterase inhibition-based biosensors for pesticide determination: A review. *Anal. Biochem. 429*, 19-31.

(18) Anitha, K., Mohan, S. V., and Reddy, S. J. (2004) Development of acetylcholinesterase silica sol-gel immobilized biosensor - an application towards oxydemeton methyl detection. *Biosens. Bioelectron. 20*, 848-856.

(19) Du, D., Chen, S., Cai, J., and Zhang, A. (2007) Immobilization of acetylcholinesterase on gold nanoparticles embedded in sol–gel film for amperometric detection of organophosphorous insecticide. *Biosens. Bioelectron. 23*, 130-134.

(20) Wong, L. S., Khan, F., and Micklefield, J. (2009) Selective Covalent Protein

Immobilization: Strategies and Applications. *Chem. Rev. 109*, 4025-4053.

(21) Andreescu, S., Bucur, B., and Marty, J.-L. (2006) Affinity Immobilization of Tagged Enzymes, *Immobilization of enzymes and cells*. (Guisan, J. M., Ed.) pp 91-106, Chapter 9, Springer.

(22) Ganesana, M., Istarnboulie, G., Marty, J.-L., Noguer, T., and Andreescu, S. (2011) Site-specific immobilization of a (His)6-tagged acetylcholinesterase on nickel nanoparticles for highly sensitive toxicity biosensors. *Biosens. Bioelectron. 30*, 43-48.

(23) Ivanov, Y., Marinov, I., Gabrovska, K., Dimcheva, N., and Godjevargova, T. (2010) Amperometric biosensor based on a site-specific immobilization of acetylcholinesterase via affinity bonds on a nanostructured polymer membrane with integrated multiwall carbon nanotubes. *J. Mol. Catal. B: Enzym. 63*, 141-148.

(24) Ivanov, Y., Marinov, I., Portaccio, M., Lepore, M., Mita, D. G., and Godjevargova, T. (2012) Flow-injection system with site-specific immobilization of acetylcholinesterase biosensor for amperometric detection of organophosphate pesticides. *Biotechnol. Biotechnol. Equip. 26*, 3044-3053.

(25) Chumphukam, O., Le, T. T., and Cass, A. E. (2014) High efficiency acetylcholinesterase immobilization on DNA aptamer modified surfaces. *Molecules 19*, 4986-96.

(26) Lalonde, J., and Margolin, A. (2008) Immobilization of Enzymes, *Enzyme*

Catalysis in Organic Synthesis pp 163-184, Chapter 6, Wiley-VCH Verlag GmbH.

(27) Nelson, D. L., Lehninger, A. L., and Cox, M. M. (2008) Enzymes, *Lehninger principles of biochemistry* pp 187-234, Chapter 6, Macmillan.

(28) Raves, M. L., Harel, M., and Pang, Y.-P. (1997) Structure of acetylcholinesterase complexed with the nootropic alkaloid,(-)-huperzine A. *Nat. Struct. Biol. 4*, 57-63.

(29) Kryger, G., Harel, M., Giles, K., Toker, L., Velan, B., Lazar, A., Kronman, C., Barak, D., Ariel, N., Shafferman, A., et al. (2000) Structures of recombinant native and E202Q mutant human acetylcholinesterase complexed with the snake-venom toxin fasciculin-II. *Acta Crystallogr., Sect. D: Biol. Crystallogr. 56*, 1385-1394.

(30) Kang, T. S., Georgieva, D., Genov, N., Murakami, M. T., Sinha, M., Kumar, R. P., Kaur, P., Kumar, S., Dey, S., Sharma, S., et al. (2011) Enzymatic toxins from snake venom: structural characterization and mechanism of catalysis. *FEBS J. 278*, 4544-4576.

(31) Levitt, M., and Chothia, C. (1976) Structural patterns in globular proteins. *Nature 261*, 552-558.

(32) Fiser, A., and Šali, A. (2003) Modeller: Generation and Refinement of Homology-Based Protein Structure Models, *Methods in Enzymology* pp 461-491, Chapter 20, Academic Press.

(33) Dvir, H., Silman, I., Harel, M., Rosenberry, T. L., and Sussman, J. L. (2010) Acetylcholinesterase: From 3D structure to function. *Chem.-Biol. Interact. 187*, 10-22.

(34) Li, D.-Z., Yu, G.-Q., Yi, S.-C., Zhang, Y., Kong, D.-X., and Wang, M.-Q. (2015) Structure-Based Analysis of the Ligand-Binding Mechanism for DhelOBP21, a C-minus Odorant Binding Protein, from Dastarcus helophoroides (Fairmaire; Coleoptera: Bothrideridae). *Int. J. Biol. Sci. 11*, 1281-1295.

(35) Irwin, J. J., Sterling, T., Mysinger, M. M., Bolstad, E. S., and Coleman, R. G. (2012) ZINC: A Free Tool to Discover Chemistry for Biology. *J. Chem. Inf. Model. 52*, 1757-1768.

(36) Ding, F., Zhao, G., Huang, J., Sun, Y., and Zhang, L. (2009) Fluorescence spectroscopic investigation of the interaction between chloramphenicol and lysozyme. *Eur. J. Med. Chem. 44*, 4083-4089.

(37) Tian, J. N., Liu, J. Q., He, W. Y., Hu, Z. D., Yao, X. J., and Chen, X. G. (2004) Probing the binding of scutellarin to human serum albumin by circular dichroism, fluorescence spectroscopy, FTIR, and molecular modeling method. *Biomacromolecules 5*, 1956-1961.

(38) Maity, M., Dolui, S., and Maiti, N. C. (2015) Hydrogen bonding plays a significant role in the binding of coomassie brilliant blue-R to hemoglobin: FT-IR, fluorescence and molecular dynamics studies. *Phys. Chem. Chem. Phys. 17*, 31216-31227.

(39) Monti, S., Manet, I., and Marconi, G. (2011) Combination of spectroscopic and computational methods to get an understanding of supramolecular chemistry of drugs: from simple host systems to biomolecules. *Phys. Chem. Chem. Phys. 13*, 20893-20905.

(40) Lakowicz, J. R. (2006) *Principles of fluorescence spectroscopy*, third ed., pp 97-330, Springer, New York.

(41) Rohacova, J., Sastre, G., Marin, M. L., and Miranda, M. A. (2011) Dansyl Labeling To Modulate the Relative Affinity of Bile Acids for the Binding Sites of Human Serum Albumin. *J. Phys. Chem. B 115*, 10518-10524.

(42) Sun, Q., Peng, D.-Y., Yang, S.-G., Zhu, X.-L., Yang, W.-C., and Yang, G.-F. (2014) Syntheses of coumarin–tacrine hybrids as dual-site acetylcholinesterase inhibitors and their activity against butylcholinesterase, Aβ aggregation, and β-secretase. *Bioorg. Med. Chem. 22*, 4784-4791.

(43) Harel, M., Schalk, I., Ehretsabatier, L., Bouet, F., Goeldner, M., Hirth, C., Axelsen, P. H., Silman, I., and Sussman, J. L. (1993) Quaternary ligand binding to aromatic residues in the active-site gorge of acetylcholinesterase. *Proc. Natl. Acad. Sci. U. S. A. 90*, 9031-9035.

(44) Cheung, J., Rudolph, M. J., Burshteyn, F., Cassidy, M. S., Gary, E. N., Love, J., Franklin, M. C., and Height, J. J. (2012) Structures of Human Acetylcholinesterase in Complex with Pharmacologically Important Ligands. *J. Med. Chem. 55*, 10282-10286.

(45) Scatchard, G. (1949) The attractions of proteins for small molecules and ions. *Ann. N. Y. Acad. Sci. 51*, 660-672.

(46) Kato, G., Yung, J., and Ihnat, M. (1970) NMR studies of the interaction of eserine and atropine with acetylcholinesterase. *Biochem. Biophys. Res. Commun. 40*, 15-&.

(47) Mach, H., Middaugh, C. R., and Lewis, R. V. (1992) Statistical determination of the average values of the extinction coefficients of tryptophan and tyrosine in native proteins. *Anal. Biochem. 200*, 74-80.

(48) Gordon, J. C., Myers, J. B., Folta, T., Shoja, V., Heath, L. S., and Onufriev, A. (2005) H++: a server for estimating pK(a)s and adding missing hydrogens to macromolecules. *Nucleic Acids Res. 33*, W368-W371.

(49) Holt, P. A., Chaires, J. B., and Trent, J. O. (2008) Molecular Docking of Intercalators and Groove-Binders to Nucleic Acids Using Autodock and Surflex. *J. Chem. Inf. Model. 48*, 1602-1615.

(50) Ellman, G. L., Courtney, K. D., Andres, V., and Featherstone, R. M. (1961) A new and rapid colorimetric determination of acetylcholinesterase activity. *Biochem. Pharmacol. 7*, 88-&.

Table of Contents Graphic

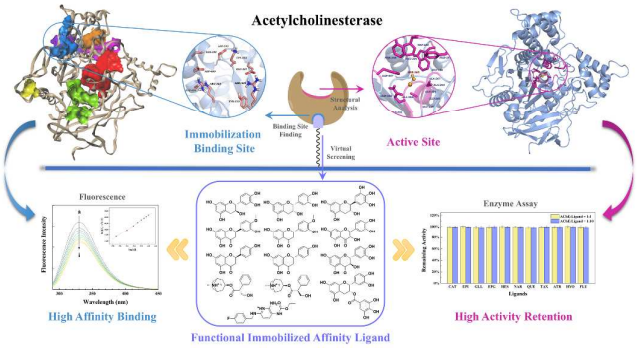

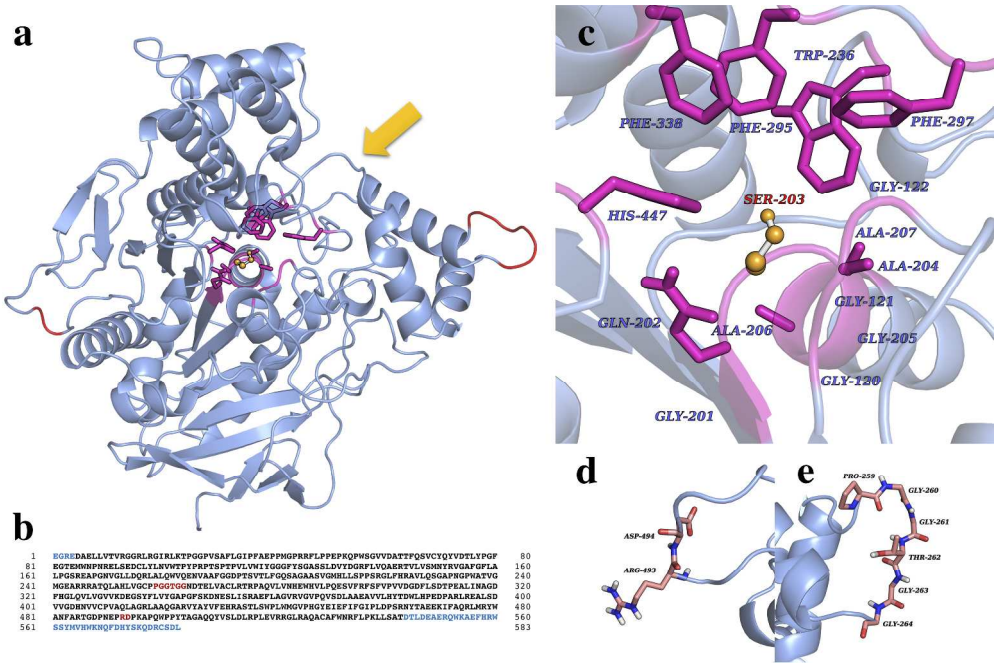

Figure 1 Three-dimensional structure of AChE. Panel (A) showed the ribbon model of acetylcholinesterase derived from x-ray crystallography (PDB: 1F8U); Red loop showed the missing loops by MODELLER; Magenta area showed the active site of AChE; Yellow arrow indicated the location of AChE's substrate channel. Panel (B) showed the amino acidic sequences of AChE. Black, existing amino acid residues in 1F8U; Red, missing amino acid residues in the middle; Blue, missing amino acid residues at the beginning or the end. Panel (C) showed the structure of the active site of AChE. Panel (D) and (E) showed the structure of the missing loops, respectively. These illustrations were made with PyMOL on the basis of the atomic coordinates available at the Brookhaven Protein Data Bank (http://www.rcsb.org/pdb).

319x209mm (300 x 300 DPI)

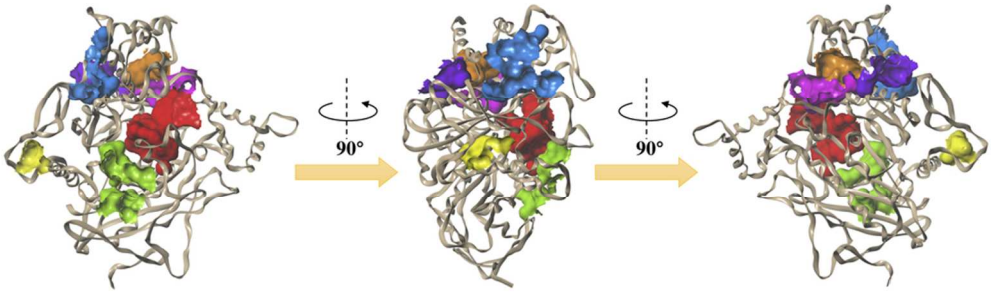

Figure 2 The cavities on the protein of AChE. The cavities included active site (red), Site1 (blue), Site2 (chartreuse), Site3 (magenta), Site4 (purple), Site5 (orange) and Site6 (yellow). These illustrations were made with Sybyl.

85x25mm (300 x 300 DPI)

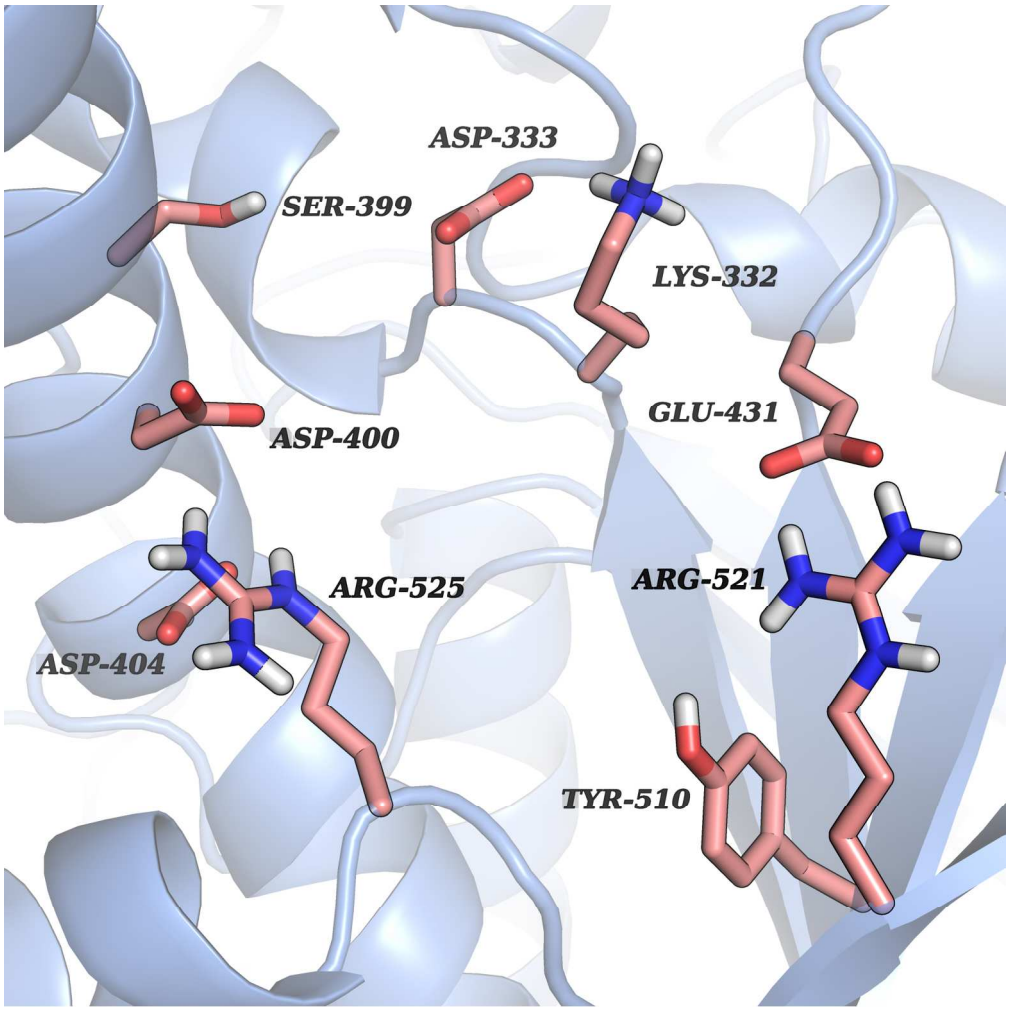

Figure 3 The structure of the immobilization site (Site1). The key amino acid residues (Lys332, Asp333, Ser399, Asp400, Asp404, Glu431, Tyr510, Arg521, Arg525) in Site1 have been shown as a stick model and colored as per the atoms. This illustration was made with PyMOL.

169x169mm (300 x 300 DPI)

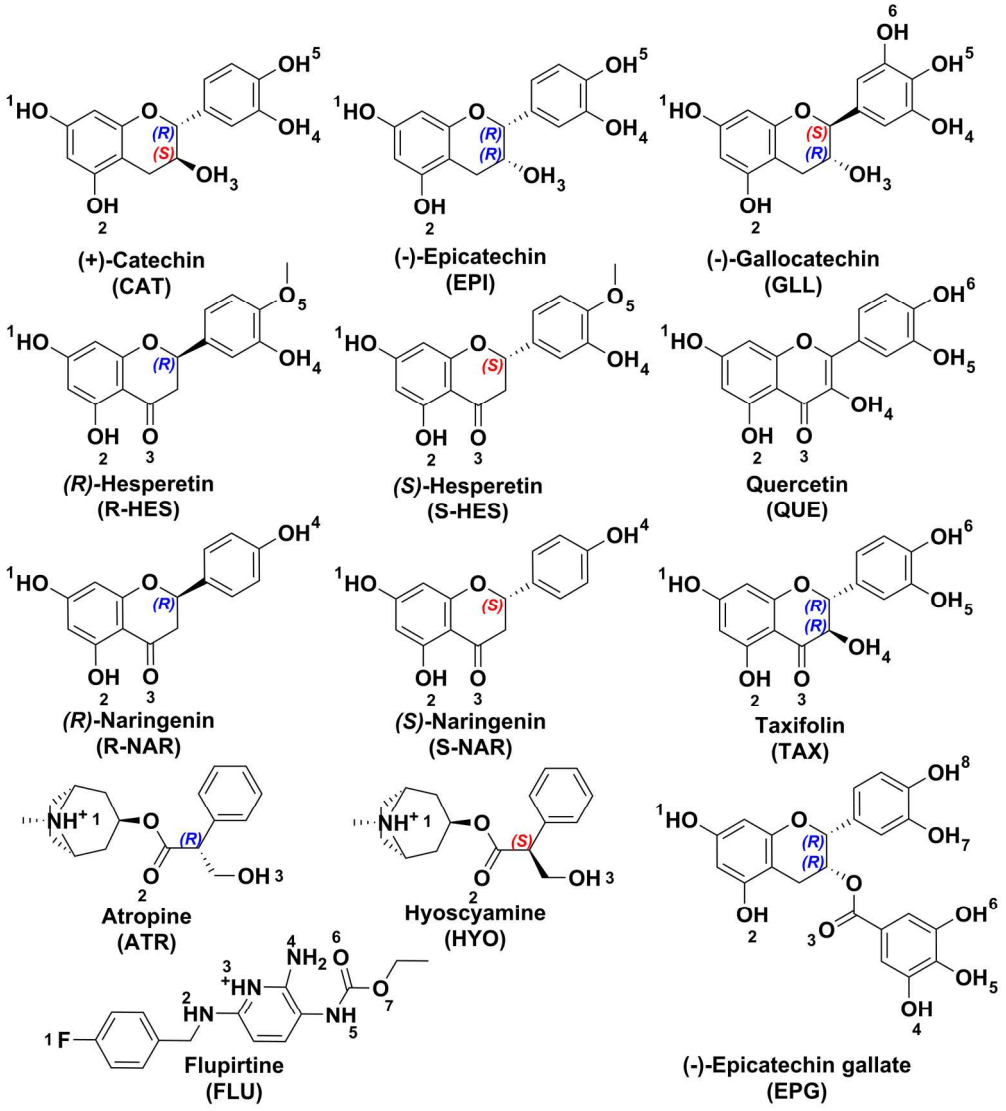

Figure 4 Molecular structure of ligands. The parts of chiral atoms of ligands were marked.

178x198mm (300 x 300 DPI)

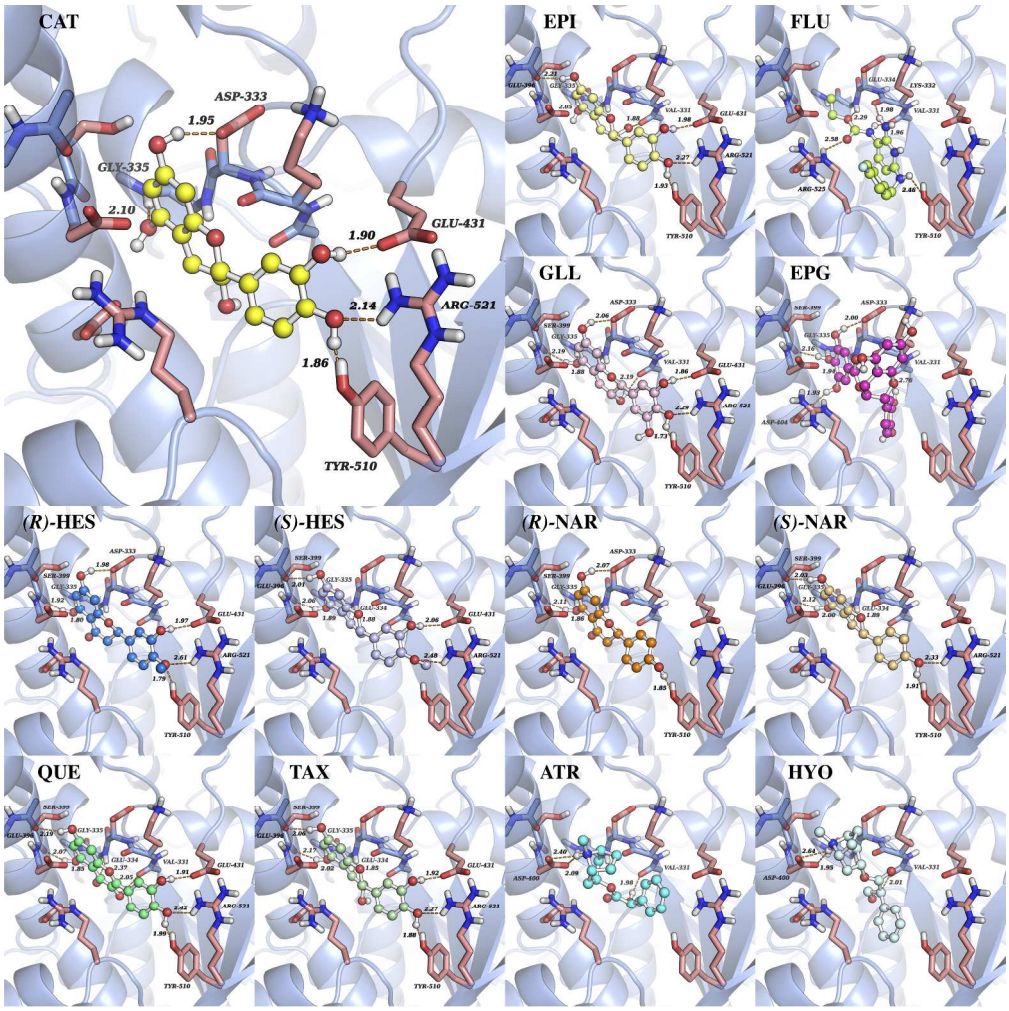

Figure 5 Molecular modeling of ligands docked to AChE. The critical amino acid residues around (+)-catechin (yellow), (-)-epicatechin (pale yellow), (-)-gallocatechin (light pink), epicatechin gallate (light magenta), (*R*)-hesperetin (marine), (*S*)-hesperetin (light blue), (*R*)-naringenin (orange), (*S*)-naringenin (light orange), quercetin (lime green), taxifolin (pale green), atropine (cyan), hyoscyamine (pale cyan) and (-)-flupirtine (limon) have been manifested in stick model form, respectively. These illustrations were made with PyMOL.

319x319mm (300 x 300 DPI)